

Spin orientation at semiconductor heterointerfaces

Bernard Jusserand

*Laboratoire de Bagneux, France Télécom, Centre National d'Etudes des Télécommunications/Paris B,
196 avenue Henri Ravera, 92220 Bagneux, France*

David Richards

Cavendish Laboratory, Madingley Road, Cambridge CB3 0HE, United Kingdom

Guy Allan and Catherine Priester

*Institut d'Électronique et de Microélectronique du Nord, Département de l'Institut Supérieur d'Electronique du Nord, Boîte Postale 79,
Villeneuve d'Ascq Cedex, France*

Bernard Etienne

*Laboratoire de Microstructures et Microélectronique, Centre National de la Recherche Scientifique,
196 avenue Henri Ravera, 92220 Bagneux, France*

(Received 24 October 1994)

We demonstrate by Raman scattering that the spin splitting in the conduction band of a GaAs/Ga_{1-x}Al_xAs asymmetric quantum well is anisotropic and inequivalent along the $[\bar{1}\bar{1}]$ and $[11]$ directions. This agrees with the results of tight-binding calculations. The Rashba contribution to the spin orientation induced by the asymmetric potential is of comparable magnitude to the bulk inversion-asymmetry-induced term. Hence, we obtain quantitative information on the origin of the spin orientation at the GaAs/Ga_{1-x}Al_xAs interface.

The spin-orbit splitting in the conduction band of semiconductors without inversion symmetry, such as GaAs, has recently attracted interest.¹⁻⁴ This spin splitting plays an essential role in the spin relaxation of carriers⁵ and is expected to influence strongly electron transport in quantum wires.⁶ Accurate experiments have been reported^{1,2,4} on high-mobility two-dimensional electron gases with large Fermi wave vectors ($k_F \approx 3.0 \times 10^6 \text{ cm}^{-1}$) confined in modulation-doped heterostructures. Using Raman scattering we have recently obtained² spectroscopic evidence, in the absence of any applied magnetic field, of this spin splitting. Reasonable agreement was obtained¹⁻⁴ between these determinations and simple perturbative extensions⁷⁻⁹ of bulk band structure¹⁰ to the case of quantum wells (QW's). These results were further supported by a recent tight-binding calculation of the spin splitting in a symmetric quantum well.³

However, it has been overlooked that, because of the sensitivity of the spin orientation of the confined electron to the presence of the GaAs/Ga_{1-x}Al_xAs interface, the determination of the spin splitting provides a valuable test of the heterostructure potential. Contrary to the situation in a symmetric QW, the electron confined in a one-side modulation-doped QW experiences an almost triangular potential well. It is thus sensitive to three different average electric fields: \mathbf{F}_b , \mathbf{F}_{SC} , and \mathbf{F}_h . The intrinsic spin splitting, due to the GaAs inversion asymmetry,^{5,10} can be understood to be due to an effective bulklike local electric field \mathbf{F}_b . As in the case of symmetric wells, the contribution due to this term is calculated in the frame of the envelope-function approximation.^{7,8} \mathbf{F}_{SC} and \mathbf{F}_h result from the doping asymmetry in the structure and give rise together to the so-called Rashba term in the spin splitting.¹¹ \mathbf{F}_{SC} is the average of the field due to the space-charge-induced band bending. The ori-

gin of \mathbf{F}_h , resulting from the potential discontinuities at the heterointerfaces, has been up to now poorly understood. Contrary to the symmetric case, the contributions of both interfaces do not cancel in asymmetric quantum wells. Within a one-band envelope-function approximation, the contribution of the heterointerface is often given as the conduction-band offset weighted by the probability density of the conduction electron at the interface.⁷ In this case, the Rashba term is negligible, as the average electric field $\boldsymbol{\varepsilon} = \mathbf{F}_{SC} + \mathbf{F}_h$ for a bound state should be close to zero. Using a multiband Hamiltonian, a similar expression for the Rashba spin splitting results,^{12,13} with the exception that the valence-band offset must be considered instead of that of the conduction band. The Rashba term then becomes large and the predicted angular anisotropy of the spin splitting is drastically modified.

We demonstrate here that Raman scattering brings significant information to this problem. Because Raman scattering is a unique probe of electronic excitations with wave vector fixed in *both magnitude and orientation*, it is possible in some experimental conditions, which we have quantitatively defined, to measure the angular anisotropy of the spin splitting in the conduction band. We get evidence of a significant, but unexpectedly small, anisotropy, and of the inequivalence of the $[\bar{1}\bar{1}]$ and $[11]$ directions in the layer plane. This gives direct proof that the magnitudes of the bulklike, and Rashba, contributions to the spin splitting are comparable. This result clearly contradicts the widely accepted model, which predicts a negligible heterostructure contribution and thus a large anisotropy and a fourfold invariance.^{8,9} We have also performed a tight-binding calculation of the spin splitting for conduction electrons confined in an asymmetric QW, compa-

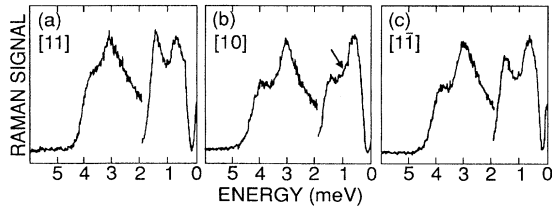


FIG. 1. Raman spectra measured in crossed polarization for \mathbf{q} parallel to $[11]$ (a), $[10]$ (b), and $[1\bar{1}]$ (c) directions and in each case for two different magnitudes $q=0.31\times 10^5\text{ cm}^{-1}$ (lower-energy curves) and $1.16\times 10^5\text{ cm}^{-1}$ (higher-energy curves). The arrow in (b) marks the emergence of an additional peak for small q .

nable to our sample. The results are consistent with our experimental findings and provide insight into the effective potential step δV relevant for the spin orientation.

The Raman-scattering experiments were performed in pumped liquid helium with incident photon energies around 1.6 eV. The sample was an asymmetrically doped 180-Å-thick single quantum well with a structure similar to those described previously.^{2,4} We focus here on the single-particle-excitation (SPE) Raman signal obtained with crossed incident and scattered polarizations, which is related to spin-flip electronic transitions. We show in Fig. 1 the Raman signal obtained for two different magnitudes and three different orientations of the transferred wave vector \mathbf{q} in the plane of the quantum well. The two peaks in each spectrum are related to the SPE transitions from the spin-up to the spin-down subbands and vice versa. For small q ($0.31\times 10^5\text{ cm}^{-1}$), very strong variations of the relative intensities of the two spin-split SPE peaks are observed as a function of the orientation. Moreover, an additional component, indicated by an arrow in Fig. 1(b), is just resolved when $\mathbf{q}\parallel[10]$. For larger q ($1.16\times 10^5\text{ cm}^{-1}$), the line shape becomes less sensitive to the orientation while small but clear shifts of the Raman peaks can be measured. In both cases, the Raman spectra for $\mathbf{q}\parallel[11]$ and $\mathbf{q}\parallel[1\bar{1}]$ are significantly different, which reflects a clear departure from the D_{2d} symmetry in our asymmetric quantum wells.

The imaginary part of the intrasubband polarizability, which essentially describes the SPE Raman line shape, reflects the joint density of states at a given wave vector \mathbf{q} , weighted by the Fermi occupation functions of the initial and final states. Assuming vanishingly small temperature and $q\ll k_F$ (a reasonable approximation in our experiments), all involved states lie very close to the Fermi surface, in which case we can describe this density of states graphically, as described below. In the presence of an anisotropic spin splitting, the energy transfer for a given initial state \mathbf{k} is

$$\Delta\Omega_{\pm} = \frac{\hbar^2}{m} qk \cos(\theta - \phi) \pm 2\Delta E(k, \theta), \quad (1)$$

where the sign $+$ ($-$) refers to the spin-down–spin-up (spin-up–spin-down) transition, and the angles θ, ϕ define the orientation of \mathbf{k} and \mathbf{q} with respect to the $[10]$ crystal axis, respectively. In Eq. (1), for fixed \mathbf{q} , the only significant variation is associated with θ because $k\approx k_F$. We show in Fig. 2 $\Delta\Omega_{+}$ and $\Delta\Omega_{-}$ as a function of θ for three different

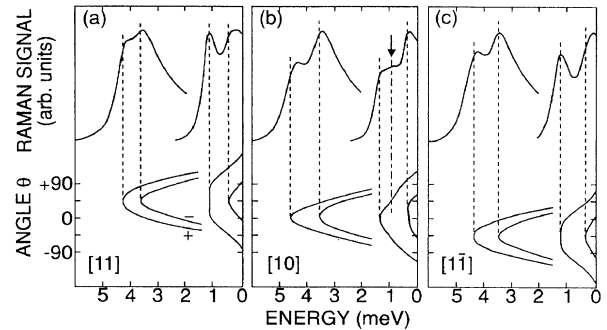


FIG. 2. For each wave-vector orientation: $[11]$ (a), $[10]$ (b), and $[1\bar{1}]$ (c), the upper traces are the Raman spectra calculated for $q=0.3\times 10^5\text{ cm}^{-1}$ (lower-energy curves) and $1.4\times 10^5\text{ cm}^{-1}$ (higher-energy curves). The peak positions are compared in each case to the high-density points in the associated $\Delta\Omega_{\pm}(k_F, \theta)$ curves (lower traces), calculated from Eq. (1).

sample orientations ϕ and the corresponding calculated Raman signals in crossed polarization, determined from the imaginary part of the intrasubband polarizability. Peaks appear in the Raman signal when $d\Delta\Omega_{\pm}/d\theta=0$. At large q (higher-energy curve), a single peak is obtained for each spin-flip transition due to the contribution of SPE from initial states around $\mathbf{k}=k_F(\mathbf{q}/q)$ with a peak separation of $4\Delta E(k=k_F, \theta=\phi)$. However, this simple description does not hold at small q (low-energy curve) because in this case $\Delta\Omega_{\pm}$ displays several different extrema for different angles θ , as the first term in Eq. (1) is not large enough to select efficiently a direction in the two-dimensional Brillouin zone. Nevertheless, from the spectra at large q we extract estimates of ΔE of 0.25 meV along $[10]$, 0.17 meV along $[11]$, and 0.22 meV along $[1\bar{1}]$. The accuracy, shown in Fig. 3, corre-

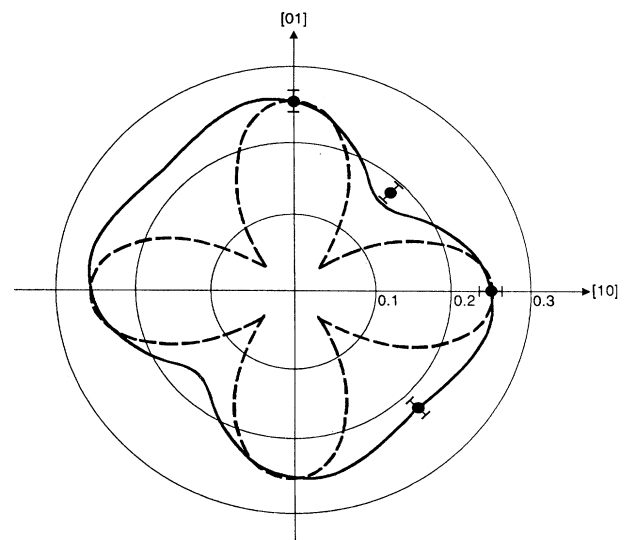


FIG. 3. Angular variation of the spin splitting due to the bulk electric field only [Eq. (2), dashed line] and to the total electric field [Eq. (6), thick lines]. The parameters have been determined as described in the text to fit the experiments (full dots).

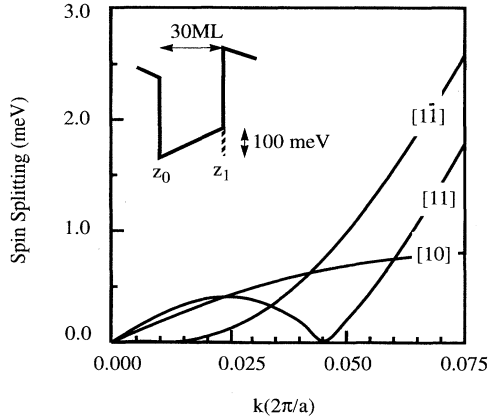


FIG. 4. Spin splitting versus wave vector k determined from tight-binding calculations of the asymmetric quantum well shown in the inset. The corresponding electric field is $F_{SC} = -1.18 \text{ mV } \text{Å}^{-1}$.

sponds to an error of $\pm 0.05 \text{ meV}$ in the experimental peak separation.

The contribution $2\Delta E_b$ of the bulklike field F_b to the spin-splitting $2\Delta E$ is given by⁴

$$\Delta E_b = a_{42} \{ \kappa^4 k_F^2 - (4\kappa^2 - k_F^2) k_F^4 \sin^2 \theta \cos^2 \theta \}^{1/2}, \quad (2)$$

where a_{42} is a material-related expansion parameter⁷ and κ^2 is the average value of the operator $-d^2/dz^2$ over the confined electron wave function. We have estimated from a self-consistent Poisson Schrödinger calculation: $\kappa = 1.85 \times 10^6 \text{ cm}^{-1}$. From the electron density, $k_F = 2.86 \times 10^6 \text{ cm}^{-1}$. As illustrated in Fig. 3, the spin splitting measured along [10] (0.25 meV) is well reproduced assuming $|a_{42}| = 27 \text{ eV } \text{Å}^3$, in reasonable agreement with available theoretical values^{4,14} ($-22 \pm 4 \text{ eV } \text{Å}^3$). However, the predicted variation of the ΔE as a function of θ is very strong, in complete disagreement with the experimental observations.

Let us now introduce the Rashba term¹¹

$$\Delta E_r = a_{64} k_F \varepsilon, \quad (3)$$

where a_{64} is a material-related expansion parameter.⁷ ε contains two terms and reads

$$\varepsilon = (F_{SC} + F_h) \mathbf{e}_z. \quad (4)$$

From our self-consistent Poisson Schrödinger calculation we find F_{SC} , the average of the space-charge field over the electron wave function, to be -1.06 mV/Å . F_h from the hetero-interfaces is

$$F_h = \delta V [|\psi|^2(z_0) - |\psi|^2(z_1)], \quad (5)$$

where δV is the potential step at the interfaces, located at z_0 and z_1 , respectively. The unit vector \mathbf{e}_z is oriented out of the sample, so that F_{SC} is negative and $z_1 < z_0$ (see inset in Fig. 4). When considering both contributions to the spin splitting together, one has to include an interference term, so that the total splitting is

$$2\Delta E = 2 \{ \Delta E_b^2 + \Delta E_r^2 + 2a_{42}a_{64}\varepsilon(2\kappa^2 - k_F^2)k_F^2 \sin \theta \cos \theta \}^{1/2}. \quad (6)$$

The fourfold symmetry is then broken by the interference term and only a twofold symmetry remains,¹⁵ as observed in our experiment. Using Eq. (6) and the three measurements of ΔE at large q and $\theta = \phi = 0, \pm 45$, we have fitted the two independent parameters: $|a_{42}| = 16.5 \pm 3 \text{ eV } \text{Å}^3$ and $|a_{64}\varepsilon| = 6.9 \pm 0.4 \text{ meV } \text{Å}$. With these values, we have reproduced well the line shape at small q , including the emergence of the third peak indicated by an arrow in Figs. 1 and 2 for $q \parallel [10]$. This overall agreement is illustrated in Figs. 1 and 2. The corresponding angular dependence of ΔE is significant but small, as shown in Fig. 3, and the angular average of both bulk and Rashba terms are comparable in magnitude. Our experiments do not provide the absolute sign of a_{42} and $a_{64}\varepsilon$ but, owing to the interference term in Eq. (6), we have determined the relative sign to be positive.

We have checked the validity of Eq. (6) with a tight-binding calculation of the spin splitting in a $\text{GaAs}_{30}/\text{AlAs}_{15}$ superlattice grown along the [001] direction. The materials are described within the semiempirical tight-binding method with a sp^3s^* basis,¹⁶ including spin-orbit coupling.¹⁷ We used the parameters of Ref. 18, which provide a correct spin splitting for GaAs. Unlike Ref. 3, we have added a constant electric field in the well and a constant opposing electric field in the barriers (in order to preserve the periodicity of the structure). The corresponding unit cell (see inset of Fig. 4) reasonably mimics our one-sided modulation-doped QW, while keeping the computation time reasonably low. When $F_{SC} = 0$, we reproduce the results of Fig. 3. When a nonvanishing field is introduced, the spin splittings along [11] and $[\bar{1}\bar{1}]$ become quite different and this difference increases with increasing electric field. We show in Fig. 4 the calculated spin splitting as a function of k , the magnitude of the wave vector in the layer plane, along [10], [11], and $[\bar{1}\bar{1}]$ for $F_{SC} = 1.18 \text{ mV } \text{Å}^{-1}$. All the results are in semiquantitative agreement with our experimental findings and justify our perturbative approach for a reasonably small wave-vector magnitude. Furthermore, our calculation suggests that a large twofold anisotropy should be observed in asymmetric quantum wells with higher Fermi wave vector.

Let us now discuss our experimental determinations of a_{42} and $a_{64}\varepsilon$. We have determined a value for a_{42} ($|a_{42}| = 16.5 \pm 3 \text{ eV } \text{Å}^3$) in good agreement with the available theoretical values ($-22 \pm 4 \text{ eV } \text{Å}^3$). This provides the absolute sign of $a_{64}\varepsilon$ so that $a_{64}\varepsilon = -6.9 \pm 0.4 \text{ meV } \text{Å}$. Even though our experiment on a single sample does not provide an independent determination of a_{64} and ε , we conclusively demonstrate that the average field ε experienced by the conduction electron is not negligible. Moreover, we have compared the predicted values for this product when considering either the valence-band offset or the conduction-band offset for δV in Eq. (5). In our sample (Al concentration $x = 0.33$), they amount to -140 and $+280 \text{ mV}$, respectively. Using these values and $F_{SC} = -1.06 \text{ mV/Å}$ and $|\psi|^2(z_0) - |\psi|^2(z_1) = 4.5 \times 10^{-3} \text{ Å}^{-1}$ determined from our self-consistent Poisson-Schrödinger calculation, we have obtained the following: $\varepsilon = -1.7 \text{ mV } \text{Å}^{-1}$ (valence-band offset) or $\varepsilon = +0.2 \text{ mV } \text{Å}^{-1}$ (conduction-band offset) and thus two alternative determinations of a_{64} : $a_{64} = +4.1$

$\pm 0.25 e\text{\AA}^2$ (valence-band offset) or $a_{64} = -34.5 \pm 2 e\text{\AA}^2$ (conduction-band offset). The valence-band-offset result compares quite favorably with the available theoretical value ($+5.5 e\text{\AA}^2$),⁷ while the conduction-band-offset model is clearly rejected. Even taking into account a more conservative uncertainty in the experimental results (± 0.1 meV) and some error in the theoretical parameters, the agreement with Eq. (6) remains good, provided that the valence-band offset is used for δV according to Refs. 12 and 13.

In the spirit of the qualitative description of the spin splitting resulting from the electron moving in an electric field, the interface contribution comes from the charge transfer at the interface. Based on the discussion in Ref. 19 of band-offset formation in semiconductor heterojunctions, there is a close connection between the charge transfer and the valence-band offset, in good agreement with our conclusions. Furthermore, one should also consider¹⁹ the potential alignment due to the charge transfer at the interface to define the potential step responsible for the spin splitting, as this

quantity reflects the average electron-charge redistribution around the interface. Using several samples with various parameters, or alternatively calculating the spin splitting within semiempirical or *ab initio* frames for various interfaces, would allow a more accurate determination of the interface contribution and a quantitative test of this description.

To conclude, we have shown in this paper that the spin splitting of the conduction band in asymmetric quantum wells is a very sensitive probe of the potential discontinuity at a heterointerface. From a detailed analysis of the SPE Raman-scattering signal, we have obtained an overall understanding of the in-plane anisotropy of this spin splitting. This provides insight into the spin-orbit coupling at the interface, which is shown to be related to the corresponding valence-band offset.

We would like to acknowledge G. Bastard, C. Dahl, G. Fasol, J. M. Gerard, H. P. Hughes, W. Knap, D. J. Lovering, and J. Y. Marzin for numerous helpful discussions. D.R. thanks St. John's College, Cambridge, for support.

-
- ¹P. D. Dresselhaus, C. M. A. Papavassiliou, R. G. Wheeler, and R. N. Sacks, *Phys. Rev. Lett.* **68**, 106 (1992).
²B. Jusserand, D. Richards, H. Peric, and B. Etienne, *Phys. Rev. Lett.* **69**, 848 (1992).
³P. V. Santos and M. Cardona, *Phys. Rev. Lett.* **72**, 432 (1994).
⁴D. Richards, B. Jusserand, H. Peric, and B. Etienne, *Phys. Rev. B* **47**, 16 028 (1993).
⁵G. E. Pikus, V. A. Marushchak, and A. N. Titkov, *Fiz. Tekh. Poluprovodn.* **22**, 185 (1988) [*Sov. Phys. Semicond.* **22**, 115 (1988)].
⁶G. Fasol and H. Sakaki, *Phys. Rev. Lett.* **70**, 3643 (1993).
⁷F. Malcher, G. Lommer, and U. Rössler, *Superlatt. Microstruct.* **2**, 267 (1986).
⁸R. Eppenga and M. F. H. Schuurmans, *Phys. Rev. B* **37**, 10 923 (1988).
⁹E. I. Rashba and E. Ya. Sherman, *Phys. Lett. A* **129**, 175 (1988).
¹⁰U. Rössler, *Solid State Commun.* **49**, 943 (1984); M. Cardona, N. E. Christensen, and G. Fasol, *Phys. Rev. B* **38**, 1806 (1988).
¹¹F. J. Ohkawa and Y. Uemura, *J. Phys. Soc. Jpn.* **37**, 1325 (1974); Y. A. Bychkov and E. I. Rashba, *J. Phys. C* **17**, 6039 (1984).
¹²R. Lassnig, *Phys. Rev. B* **31**, 8076 (1985).
¹³R. Winkler and U. Rössler, *Phys. Rev. B* **48**, 8918 (1993).
¹⁴H. Mayer and U. Rössler, *Solid State Commun.* **87**, 81 (1993).
¹⁵E. A. de Andrada e Silva, *Phys. Rev. B* **46**, 1921 (1993).
¹⁶P. Vogl, H. Hjalmarsen, and J. Dow, *J. Phys. Chem. Solids* **44**, 365 (1983).
¹⁷K. C. Hass, H. Ehrenreich, and B. Velicky, *Phys. Rev. B* **27**, 1088 (1983).
¹⁸J. N. Schulman and Yia-Chung Chang, *Phys. Rev. B* **31**, 2056 (1985).
¹⁹S. Baroni, R. Resta, A. Baldereschi, and M. Peressi, in *Spectroscopy of Semiconductor Microstructures*, edited by G. Fasol, A. Fasolino, and P. Lugli (Plenum, New York, 1989), p. 251; A. Baldereschi, S. Baroni, and R. Resta, *Phys. Rev. Lett.* **61**, 734 (1988).